International Journal of Thermophysics, Vol. 26, No. 4, July 2005 (© 2005)
DOI: 10.1007/s10765-005-6709-5

Homogeneity in a Metal Wire under Melting[1]

S. I. Tkachenko,[2,3] K. V. Khishchenko,[2] and P. R. Levashov[2]

Results of numerical simulations of the melting wave in a tungsten wire heated by a high-power nanosecond current pulse are presented. To take into account the hydrodynamic effects under melting, a semiempirical multiphase equation of state for tungsten is used. The structure of the melting wave at different parameters of the heating is studied, and a theoretical evaluation for the thickness of this wave, δ_m, is proposed. The homogeneity of the distribution of parameters over the wire can be expected in the case of $\delta_m \gg a_0$, where a_0 is the initial radius of the wire. The melting wave can be considered as a discontinuity of thermophysical properties of the solid and liquid phases at $\delta_m \ll a_0$.

KEY WORDS: equation of state; high-power current pulse; homogeneity; melting wave; thermophysical properties; tungsten; wire explosion.

1. INTRODUCTION

Fast heating of metal wires by a high-power current pulse is a common way for investigations of thermophysical properties of liquid metals at high pressures and temperatures [1]. Parameters of the circuit and the heated wire are usually chosen so that the skin-layer thickness is greater than the initial radius of the wire. Therefore, one can assume that parameters of the specimen possess homogeneous radial distribution during heating of the wire. Melting of the wire is initiated at the outer boundary because the energy barrier of heterogeneous nucleation of liquid on the solid specimen surface equals zero [2, 3]. This phase transition does not have to lead to a

[1] Paper presented at the Seventh International Workshop on Subsecond Thermophysics, October 6–8, 2004, Orléans, France.

[2] Institute for High Energy Densities, Russian Academy of Sciences, Izhorskaya 13/19, Moscow 125412, Russia.

[3] To whom correspondence should be addressed. E-mail: svt@ihed.ras.ru

0195-928X/05/0700-1167/0 © 2005 Springer Science+Business Media, Inc.

strong change of matter properties. In this work we have investigated the melting wave structure and the distribution of thermophysical properties of metal under subsecond explosion of tungsten wires.

2. MELTING WAVE

There are many modern investigations of the melting process under the influence of powerful fluxes of energy (see, for example, Refs. 4 and 5), but studies of the inner structure of the melting wave have not been carried out. Commonly the melting wave is considered as a discontinuity of thermophysical properties [6]. Nevertheless, it is reasonable to assume that the inner structure of the melting wave for the case of a small size specimen would be important. In this case the size of the specimen would be either comparable with or greater than the thickness of the melting wave. Under these conditions, it is necessary to take into account that a two-phase solid–liquid mixture in the melting wave should be described as a heterogeneous medium with effective properties.

Let us explain how we understand the idea 'melting wave.' This object has front and rear surfaces. The front of the melting wave is a boundary between the solid and two-phase solid–liquid mixture states of matter, whereas its rear surface is a boundary between the two-phase solid–liquid mixture and liquid states. The thickness of the melting wave, δ_m, is the distance between the front and rear surfaces; it can be much greater than the specimen size in the direction of the wave propagation.

For the case of melting of the wire heated by a large power current pulse, the nonhomogeneous distribution of parameters in the wire will be more marked for small values of the thickness, $\delta_m \lesssim a_0$, where a_0 is the initial radius of the wire. The distribution of parameters over the wire will be practically uniform during the melting process at $\delta_m \gg a_0$.

If the distributions of density and temperature over the wire are homogeneous, the pressure can be written as follows:

$$P(r) = P(a) + \tfrac{1}{4}\mu j^2 a^2 \left(1 - r^2/a^2\right), \tag{1}$$

where a is the wire radius, $P(a)$ is the ambient pressure, μ is the absolute magnetic permeability, and j is the current density. Using the technique presented in Ref. 7, we can obtain for the melting temperature increase along the wire radius,

$$\Delta T_m = (dT_m/dP)|dP| = \tfrac{1}{2}\,(dT_m/dP)\,\mu\, j^2 r\, dr, \tag{2}$$

where dT_m/dP is the temperature difference versus pressure along the melting curve. From the energy balance $c\rho dT_m/dt = j^2/\sigma_w$ (here c is the

specific heat, ρ is the density, and σ_w is the electrical conductivity), the velocity of the melting wave front v_m can be estimated according to

$$v_m = \frac{dr}{dt} = \frac{2}{\mu r \sigma_w c\rho \, (dT_m/dP)}. \tag{3}$$

We can see that the melting wave velocity depends on the distance from the wire axis and $v_m \to \infty$ at $r \to 0$. In the vicinity of the axis, boundary conditions of the symmetry are realized and then $\Delta T_m \to 0$. Therefore, volumetric isothermal melting with infinite propagation velocity takes place in this region. Such a conclusion about infinite propagation velocity is valid for any phase transition waves in the vicinity of both the symmetry axis in a cylindrical geometry and the symmetry plane in Cartesian geometry. These waves do not transfer energy or mass; therefore, it is not unusual that their velocities can reach very large values. If the distribution of the density or temperature over a specimen would be nonhomogeneous, the velocity of the phase transition wave would be limited, for example, by heat or magnetic field diffusion. Therefore, the velocity of such waves can be very small [8].

The time necessary for the melting process to be completed in a given specimen layer can be estimated from the ratio of the melting heat and the power of energy input,

$$\tau_m = \frac{\sigma_w \rho \lambda}{j^2}, \tag{4}$$

where λ is the specific heat of melting. Following that, the thickness of the melting wave can be determined as

$$\delta_m = v_m \tau_m = \frac{2\lambda}{\mu \, j^2 r \, c \, (dT_m/dP)}. \tag{5}$$

Thus, we can determine the condition of homogeneity of the distribution of wire parameters along the radius during melting, $\delta_m \gg a_0$. For evaluation of δ_m from Eq. (5), one can take $r \sim a_0$, $j \sim j_m$, and $c \sim c_m$, where j_m and c_m are typical values of the current density and specific heat in a metal just before melting. The melting wave can be considered as a discontinuity of thermophysical properties of the solid and liquid phases if the condition $\delta_m \ll a_0$ is valid.

To illustrate these theoretical evaluations, we carried out a numerical simulation of the melting wave in a tungsten wire heated by a high-power nanosecond current pulse. As one can see from Eqs. (3) and (5), the velocity and thickness of the melting wave depend on the thermodynamic parameters of the substance as well as the heating power; therefore, in the

simulations we used equation of state [9] and electrical conductivity [10, 11] models that adequately describe the thermophysical properties of the substance.

3. MODELING

In this work we investigate the initial stage of the wire heating which precedes an abrupt increase of the wire radius. Consequently, we do not take into account the axial and azimuthal nonhomogeneous effects. These effects will have influence upon the modeling results only at the later stage of the process.

If the time for thermal relaxation of an electron and lattice is less than the typical time of the process, we can assume that ion and electron temperatures are the same. In accordance with theoretical investigations [12], the time for energy relaxation under superfast heating is $\tau \sim 1$ ps for most metals in a condensed state. These data are confirmed by experiments on the interaction of a femtosecond laser pulse with metals [13].

As the Joule energy continuously affects the specimen during electrical heating, the typical value of the ion-electron relaxation time under such conditions can differ from that in experiments with short laser pulses. In accordance with theory [14, 15], a difference of electron and ion temperatures is insignificant for regimes with a typical time $\tau_c \geqslant 10$ ns. For example, we can estimate this difference for a current density $j_0 \sim 0.1\,\mathrm{TA} \cdot \mathrm{m}^{-2}$,

$$\alpha_t = \frac{\theta - T}{T} \sim \frac{e^2 j_0^2}{6(\sigma_0/l)^2 m_\mathrm{e} v_\mathrm{s}^2 \varepsilon_0} \sim 10^{-3}, \tag{6}$$

where $\varepsilon_0 = 0.5(3n_\mathrm{e}\pi^2)^{2/3}\hbar^2/m_\mathrm{e} = 3 \times 10^{-19}$ J is the Fermi energy for tungsten; T is the temperature of heavy particles; θ is the electron temperature; $\theta \sim T \sim 10$ kK is the typical value of the wire temperature immediately before explosion; $l \sim 1$ nm is the electron free path; $m_\mathrm{e} v_\mathrm{s}^2 \sim 10^{-23}$ J is the kinetic energy of the electron moving with the sound velocity; m_e is the electron mass; v_s is the sound velocity; n_e is the electron particle density; and $\sigma_0 = 0.7\,\mu\Omega^{-1} \cdot \mathrm{m}^{-1}$ is the electrical conductivity of liquid tungsten.

In this case the deviation from Ohm's law is also negligible [14];

$$\frac{\sigma_0 - \sigma_\mathrm{e}}{\sigma_0} = \frac{\pi^2}{12} (kT/\varepsilon_0)^2 (1 + \alpha_t)^2 \sim 10^{-2}, \tag{7}$$

where σ_e is the electrical conductivity of the metal while taking into account a difference of the electron and ion temperatures; k is the Boltzmann constant.

Thus, the one-temperature one-dimensional (1-D) magneto-hydrodynamic (MHD) model [16] can describe the initial stage of a wire explosion. Assuming that spatial disturbances of the wire form are small, we can write the set of equations for simulating the resistive stage of the wire heating in Lagrangian form,

$$\frac{dm}{dt} = 0, \tag{8}$$

$$\rho \frac{dv}{dt} = -\frac{\partial P}{\partial r} - \left(2\mu r^2\right)^{-1} \partial \left(r^2 B_\varphi^2\right)/\partial r, \tag{9}$$

$$\rho \frac{d\varepsilon}{dt} = -P \frac{\partial (rv)}{\partial r} + r^{-1} \frac{\partial (\kappa r \partial T/\partial r)}{\partial r} + \frac{j^2}{\sigma_w}, \text{ and} \tag{10}$$

$$\frac{d\left(\mu B_\varphi\right)}{dt} = \frac{\partial \left[(\sigma_w r)^{-1} \partial \left(r B_\varphi\right)/\partial r\right]}{\partial r}, \tag{11}$$

where v, m, ρ, and T are the velocity and the specimen mass, density, and temperature, respectively; $\varepsilon(\rho, T)$ and $P(\rho, T)$ are the specific internal energy and pressure; B_φ is the magnetic induction; $\sigma_w(\rho, T)$ and $\kappa(\rho, T)$ are the electrical and thermal conductivities; and $j = (\mu r)^{-1} \partial (r B_\varphi)/\partial r$ is the current density. The heating current $I = I(t)$ is determined by the equation describing the electric circuit,

$$\frac{d^2(L\,I)}{dt^2} + \frac{d(R_l\,I)}{dt} + \frac{I}{C} = 0, \tag{12}$$

where L is the inductance; C is the capacitance of the capacitor; and R_l is the resistance of the specimen. For the case $\delta_s \ll a$, where δ_s is the thickness of the skin layer, the value of R_l is calculated from the equation,

$$R_l(t) = l \left[2\pi \int_0^a \sigma_w r dr\right]^{-1}, \tag{13}$$

where l is the wire length. The initial and boundary conditions for Eqs. (8)–(12) are the same as in Ref. 16.

We used a semi-empirical wide-range equation of state for tungsten [9], which takes into account the effects of high-temperature melting and evaporation. This multi-phase equation of state based on the model [17–19] agrees with the collection of experimental data on static and shock

compression as well as on adiabatic and isobaric expansion of the metal; see details in Refs. 9 and 20.

The electrical conductivity of tungsten is defined by the semi-empirical formula [10],

$$\sigma_w(\rho, T) = \sigma_0 \frac{(\rho/\rho_0)^\delta}{1+\beta(T-T_0)}. \tag{14}$$

We chose the parameters $\rho_0 = 19.224\,\mathrm{g\cdot cm^{-3}}$, $T_0 = 293\,\mathrm{K}$ for the solid phase and $\rho_0 = 17.2\,\mathrm{g\cdot cm^{-3}}$, $T_0 = 3685\,\mathrm{K}$ for the liquid phase in accordance with equation-of-state reference points at atmospheric pressure, $\sigma_0 = 20.6\,\mu\Omega^{-1}\cdot\mathrm{m}^{-1}$, $\beta = 6.5\,\mathrm{kK}^{-1}$, and $\delta = 1.76$ for solid tungsten according to experimental data [1, 10] and $\sigma_0 = 0.7\,\mu\Omega^{-1}\cdot\mathrm{m}^{-1}$, $\beta = 0.02\,\mathrm{kK}^{-1}$, and $\delta = 0.67$ for liquid tungsten from data analysis [11]. The electrical conductivity of the two-phase state in the melting region is determined by

$$\sigma_{\mathrm{ef}} = \nu\sigma_{\mathrm{s}} + (1-\nu)\sigma_{\mathrm{l}}, \tag{15}$$

where σ_{s} and σ_{l} are the electrical conductivities of the solid and liquid phases, respectively, and ν is the mass concentration of the solid phase,

$$\nu(\rho, T) = \frac{\rho_{\mathrm{m}}^{-1}(T) - \rho^{-1}}{\rho_{\mathrm{m}}^{-1}(T) - \rho_{\mathrm{s}}^{-1}(T)}. \tag{16}$$

ρ_{s} and ρ_{m} are the densities of the solid and liquid phases on the melting curve.

The thermal conductivity is calculated according to the Wiedemann–Franz law,

$$\kappa(\rho, T) = k_{\mathrm{WF}} T \sigma_w(\rho, T), \tag{17}$$

where $k_{\mathrm{WF}} = (\pi^2/3)(k/e)^2$ is the Wiedemann–Franz constant.

4. NUMERICAL METHOD AND TESTING

We apply a finite-difference approximation for the set of Eqs. (8)–(11) using common approximation techniques [21, 22] of the order $O(\tau + h^2)$. Thermodynamic parameters and the current density $(\rho, T, \sigma, \varepsilon, j)$ were placed into the cells and the velocity and magnetic induction (v, B_φ) in the nodes of the grid. We used an implicit scheme to avoid rigid limitation on the time step.

To verify our computational method, we used a number of tests. We simulated the movement of a piston in a van-der-Vaals medium with a constant specific heat and compared the results with the self-consistent

solution [23]. It was shown that the numerical solutions are in good agreement with both the shock wave (piston pushed into medium) and Riemann wave (piston pulled out from medium) [23].

In order to test our numerical method for the set of MHD Eqs. (8)–(11), another test was developed. For the case of a slightly nonuniform distribution of parameters over the wire, we can write as in Ref. 23:

$$\rho(r,t)=\bar{\rho}(t)+\delta\rho(r,t), \qquad \varepsilon(r,t)=\bar{\varepsilon}(t)+\delta\varepsilon(r,t), \tag{18}$$

$$v(r,t)=r\bar{v}(t)+\delta v(r,t), \qquad B_\varphi(r,t)=r\bar{B}(t)+\delta B_\varphi(r,t), \tag{19}$$

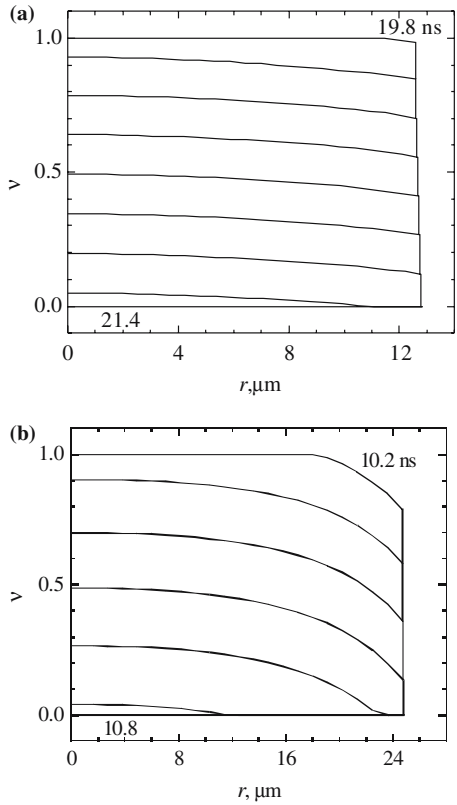

Fig. 1. Radial-dependent mass concentration of the solid phase for (a) regime 1 from $t = 19.8$ ns (upper curve) to 21.4 ns (lower curve) and (b) for regime 2 from $t = 10.2$ ns (upper curve) to 10.8 ns (lower curve). Time intervals between neighboring curves are (a) 0.2 ns and (b) 0.1 ns.

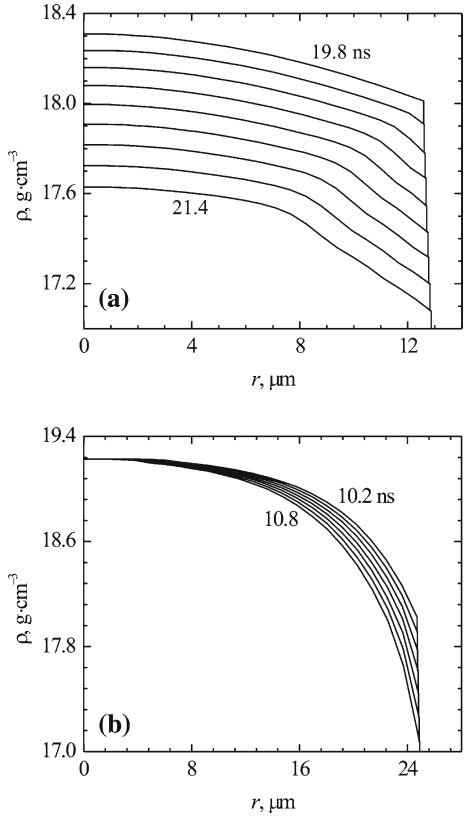

Fig. 2. Radial-dependent density of the wire for (a) regime 1 from $t = 19.8$ ns (upper curve) to 21.4 ns (lower curve) and (b) for regime 2 from $t = 10.2$ ns (upper curve) to 10.8 ns (lower curve). Time intervals between neighboring curves are (a) 0.2 ns and (b) 0.1 ns.

where $\delta\rho(r,t)/\bar{\rho}(t) \ll 1$, $\delta\varepsilon(r,t)/\bar{\varepsilon}(t) \ll 1$, $\delta v(r,t)/r\bar{v}(t) \ll 1$, $\delta B_\varphi(r,t)/r\bar{B}(t) \ll 1$. In this case at $\delta\rho(r,t) = 0$, $\delta\varepsilon(r,t) = 0$, $\delta v(r,t) = 0$, $\delta B_\varphi(r,t) = 0$, and $\bar{B}(t) = 0$, the set of Eqs. (8)–(11) has the analytical solution,

$$\rho_a = \rho_d/(D+At)^2, \quad v_a = Ar/(D+At), \quad T_a = T_d\left[(D+At)^2 - b\rho_d\right]^{-R/C_v}, \quad (20)$$

where D, A, T_d and ρ_d are the parameters [23], C_v is the molar heat capacity at constant volume, and R is the universal gas constant.

We simulated two processes: 1-D radial compression ($D/A < 0$) and expansion ($D/A > 0$) of a van-der-Vaals liquid cylinder. To present

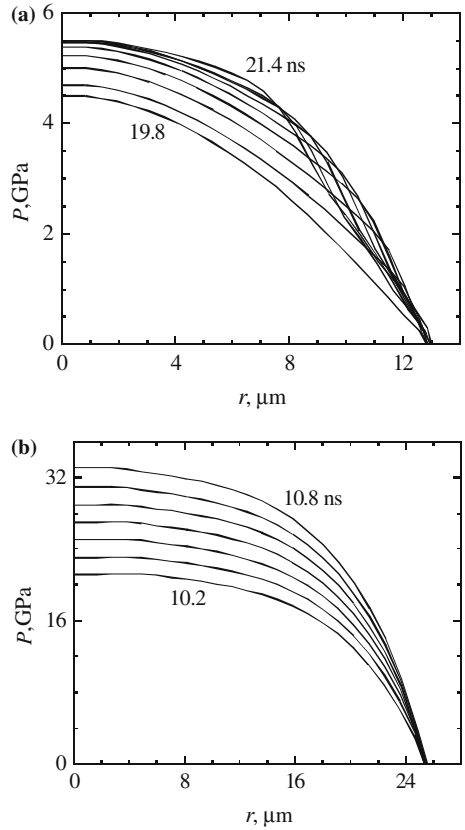

Fig. 3. Radial-dependent pressure in the wire for (a) regime 1 from $t = 19.8$ ns (lower curve) to 21.4 ns (upper curve) and for (b) regime 2 from $t = 10.2$ ns (lower curve) to 10.8 ns (upper curve). Time intervals between neighboring curves are (a) 0.2 ns and (b) 0.1 ns.

comparisons of the numerical solution with the analytical one, we used the following notations for local (the maximum value) and total (the sum over all cells or nodes) discrepancies over the computational domain: $\delta_C f = \|(f_s - f_a)/f_a\|_C$ and $\Delta_L f = \|(f_s - f_a)/f_a\|_L$, respectively; f_s and f_a are the simulated and analytical values of the corresponding function f.

Results of comparison for compression up to factor 10 are as follows: $\delta_C \rho \sim 10^{-11}, \delta_C T \sim 0.05, \delta_C v \sim 10^{-11}, \Delta_L \varepsilon \sim 0.06, \Delta_L (mv) \sim 10^{-11}$, and $\Delta_L E \sim 0.06$; $E = \varepsilon + 0.5\rho v^2 + B_\varphi/8\pi$ is the total energy. Discrepancies in the case of expansion up to a factor of four are as follows: $\delta_C \rho \sim$

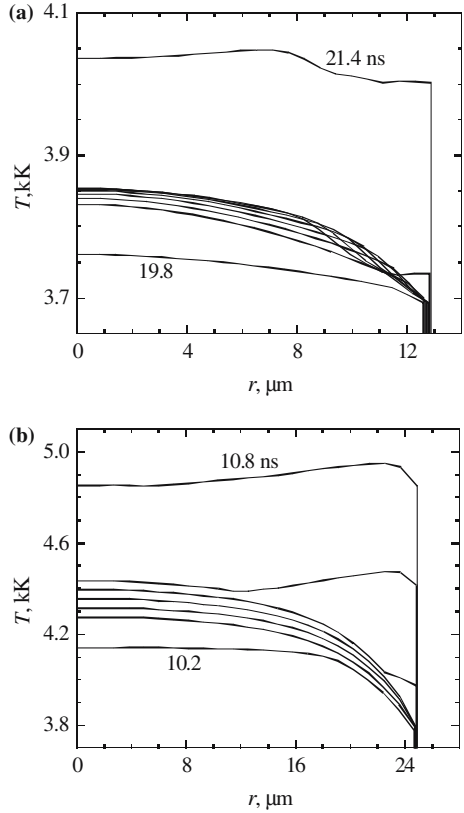

Fig. 4. Radial-dependent temperature of the wire for (a) regime 1 from $t = 19.8$ ns (lower curve) to 21.4 ns (upper curve) and for (b) regime 2 from $t = 10.2$ ns (lower curve) to 10.8 ns (upper curve). Time intervals between neighboring curves are (a) 0.2 ns and (b) 0.1 ns.

10^{-11}, $\delta_C T \sim 0.02$, $\delta_C v \sim 10^{-10}$, $\Delta_L \varepsilon \sim 0.02$, $\Delta_L(mv) \sim 10^{-11}$, and $\Delta_L E \sim 0.02$.

The results of the comparisons confirm the reliability of the presented model to simulate complex problems with a real equation of state for the medium.

5. RESULTS OF SIMULATIONS

The computer simulation of wire heating by the large power current pulse was carried out for the following parameters of tungsten wire and

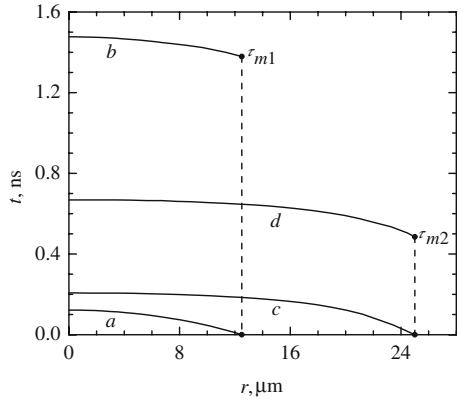

Fig. 5. The diagram, plotted as time versus radius, for propagation of the front (a, c) and rear (b, d) surfaces of melting wave into the heated wire for regimes 1 (a, b) and 2 (c, d). Time is counted off from the moment of the beginning of melting.

the electric circuit: $a_0 = 12.5\,\mu\text{m}$, $l = 12\,\text{mm}$, $L = 340\,\text{nH}$, $C = 100\,\text{nF}$, and $U_0 = 20\,\text{kV}$ (regime 1) and $a_0 = 25\,\mu\text{m}$, $l = 12\,\text{mm}$, $L = 340\,\text{nH}$, $C = 100\,\text{nF}$, and $U_0 = 200\,\text{kV}$ (regime 2); U_0 is the initial capacitor voltage. Parameters of regime 1 correspond to experiments presented in Ref. 24 and parameters of regime 2 are chosen in order to increase the current rate value; current rates are $\dot{I} \sim 60$ and $600\,\text{A}\cdot\text{ns}^{-1}$ for regimes 1 and 2, respectively.

The calculated radial distribution of the mass concentration of the solid phase, density, pressure, and temperature as a function of time are shown in Figs. 1–4 for both regimes.

In Fig. 1 are presented the radial distributions of the mass concentration of the solid phase for different moments during the melting process. The melting wave thickness exceeds the radius of the heated wire in both regimes; nevertheless, it can be assumed that $\delta_\text{m} \gg a_0$ in regime 1 and $\delta_\text{m} \sim a_0$ in regime 2. The divergences of the parameters along the wire radius during melting in regime 1 are $\Delta\nu \approx 0.08$, $\Delta\rho/\rho \approx 0.03$, and $\Delta T/T \approx 0.03$ and the maximum pressure is $P_\text{max} \approx 5.5\,\text{GPa}$; in regime 2 these parameters are as follows: $\Delta\nu \approx 0.26$, $\Delta\rho/\rho \approx 0.11$, $\Delta T/T \approx 0.1$, and $P_\text{max} \approx 33\,\text{GPa}$.

According to Eqs. (3)–(5), $\delta_{\text{m}1}/a_0 \sim 40$ and $\tau_{\text{m}1} \sim 1.4\,\text{ns}$ for regime 1, $\delta_{\text{m}2}/a_0 \sim 7$ and $\tau_{\text{m}2} \sim 0.5\,\text{ns}$ for regime 2, and $v_\text{m} \sim 10^5\,\text{m}\cdot\text{s}^{-1}$ at the initial moment of melting. Fig. 5 illustrates propagation of the melting wave into the heated wire. One can see that numerical results are in good agreement with theoretical estimations for τ_m and v_m.

It is clearly seen in Figs. 3 and 4 that the radial distributions of pressure and temperature have similar shapes during melting. This correlation of temperature and pressure at the phase transition can be explained by the fact that these values are not independent along the melting curve.

6. CONCLUSIONS

An evaluation for the thickness of a melting wave δ_m in a wire heated by a high-power current pulse is proposed. This parameter defines the condition for the homogeneity of density and temperature distributions along the radius of the wire during the phase transition, $\delta_m \gg a_0$. The melting wave can be considered as a discontinuity of thermophysical properties of the solid and liquid phases of metal at very high current densities only, when $\delta_m \ll a_0$. Excluding the last case, the inner structure of the melting wave should be taken into account when modeling the fast heating of a wire.

ACKNOWLEDGMENTS

This work was supported by the Russian Foundation for Basic Research, Grants 04-02-17292 and 05-02-17533, and the Russian Science Support Foundation, grants for talented young researchers.

REFERENCES

1. G. R. Gathers, *Rep. Progr. Phys.* **49**:341 (1986).
2. J. Frenkel, *Kinetic Theory of Liquids* (Oxford University Press, New York, 1946).
3. L. D. Landau and E. M. Lifshits, *Statistical Physics* (Pergamon Press, Oxford, 1980).
4. P. V. Breslawskii, V. I. Mazhukin, and A. A. Samokhin, *Dokl. Akad. Nauk SSSR* **320**:1088 (1991).
5. K. Sokolowskii-Tinten, J. Bialkowski, M. Boing, A. Cavalleri, and D. von der Linde, *Phys. Rev. B* **58**:R11805 (1998).
6. H. S. Carslaw and J. C. Jaeger, *Conduction of Heat in Solids* (Clarendon Press, Oxford, 1959).
7. S. I. Tkachenko and N. I. Kuskova, *J. Phys.: Condens. Mater* **11:**2223 (1999).
8. S. I. Anisimov, Ya. A. Imas, G. S. Romanov, and Yu. V. Khodyko, *Action of High-Power Radiation on Metals* (National Technical Information Service, Springfield, Virginia, 1971).
9. I. V. Lomonosov, V. E. Fortov, K. V. Khishchenko, and P. R. Levashov, in *Shock Compression of Condensed Matter — 2001*, M. D. Furnish, N. N. Thadhani, and Y. Horie, eds. (AIP, New York, 2002), pp. 111–114.
10. H. Knoepfel, *Pulsed High Magnetic Fields* (North Holland, Amsterdam, 1970).
11. N. I. Kuskova, S. I. Tkachenko, and S. V. Koval, *J. Phys.: Condens. Matter* **9:**6175 (1997).
12. P. B. Allen, *Phys. Rev. Lett.* **59**:1460 (1987).

13. S. D. Brorson, A. Kazeroonian, J. S. Moodera, D. W. Face, T. K. Cheng, E. P. Ippen, M. S. Dresselhaus, and G. Dresselhaus, *Phys. Rev. Lett.* **64**:2172 (1990).
14. V. L. Ginsburg and V. P. Shabanskii, *Dokl. Akad. Nauk SSSR* **100:**445 (1955).
15. V. P. Shabanskii, *Zh. Eksp. Teor. Fiz.* **27**:142 (1954).
16. K. V. Khishchenko, S. I. Tkachenko, P. R. Levashov, I. V. Lomonosov, and V. S. Vorob'ev, *Int. J. Thermophys*. **23**:1359 (2002).
17. A. V. Bushman and V. E. Fortov, *Sov. Tech. Rev. B: Therm. Phys.* **1:**219 (1987).
18. A. V. Bushman, V. E. Fortov, G. I. Kanel', and A. L. Ni, *Intense Dynamic Loading of Condensed Matter* (Taylor and Francis, Washington, 1993).
19. V. E. Fortov, K. V. Khishchenko, P. R. Levashov, and I. V. Lomonosov, *Nucl. Instr. Meth. Phys. Res. A* **415:**604 (1998).
20. S. I. Tkachenko, K. V. Khishchenko, V. S. Vorob'ev, P. R. Levashov, I. V. Lomonosov, and V. E. Fortov, *High Temp.* **39**:674 (2001).
21. A. A. Samarskii and Yu. P. Popov, *Raznostnye Metody Resheniya Zadach Gazovoi Dinamiki* (Difference Methods of Solving Gas-Dynamics Problems) (Nauka, Moscow, 1980).
22. V. A. Gasilov and, S. I. Tkachenko, *Differentsial'nye Uravneniya* **25**:1200 (1989).
23. S. I. Tkachenko, *Matematicheskoe Modelirovanie* **7(1)**:3 (1995).
24. S. I. Tkachenko, S. A. Pikuz, T. A. Shelkovenko, A. V. Agafonov, S. Yu. Guskov, G. V. Ivanenkov, A. R. Mingaleev, V. M. Romanova, and A. E. Ter-Oganesyan, *31st EPS Conference on Plasma Physi*cs (London, 28 June–2 July 2004) ECA, Vol. 28G, P-2.025 (2004).